

1-Ethyl-5-mercapto-1H-tetrazole as a Copper Corrosion Inhibitor in H₂SO₄ Solution

Feifei Huang¹, Xiuquan Yao^{1,*}, Xiaofang Luo²

¹ National Center for Materials Service Safety, University of Science and Technology Beijing, Beijing, 100083, P.R. China

² China Chongqing Academy of Metrology and Quality Inspection, Chongqing, 402160, P.R. China
Corresponding author.

*E-mail: b20180439@xs.ustb.edu.cn

Received: 31 December 2021 / Accepted: 28 January 2022 / Published: 4 March 2022

This work explores the use of a common molecule on pharmaceuticals, 1-Ethyl-5-Mercapto Tetrazole (EMTT), to protect copper in 0.5M H₂SO₄ solution. The addition of EMTT in sulfuric acid solution was verified to be protective of copper by testing electrochemistry, with a maximum inhibition efficiency of 88.30% at 200 mg/L. The electrochemical results were supported by the results of the surface morphology of copper specimen immersed. Finally, quantum chemical calculations were carried out to explain the retarding effect mechanistically.

Keywords: Copper; Corrosion inhibitor; Sulfuric acid solution; Electrochemistry; DFT calculation

1. INTRODUCTION

Copper is one of the most commonly used metal materials in industrial production. Copper-based alloys are widely utilized for their excellent electrical and thermal conductivity, ease of fabrication and joining, mechanical properties, and resistance to biofouling. However, corrosion of copper is a common and expensive industrial problem that can cause a certain degree of damage to the performance and appearance of copper [1, 2]. Therefore, in how to inhibit copper corrosion is a subject of great significance and deserves to be studied in depth [3, 4].

Generally speaking, one of the effective methods regarding the inhibition of copper corrosion is the addition of corrosion inhibitors [5-9]. This approach has many advantages, such as simplicity, fast and practicality. Some organic compounds containing nitrogen, phosphorus and sulfur atoms, such as phthalazine [10], Schiff bases, imidazole [11, 12], triazoles [13, 14], tetrazoles [15, 16], indazoles [17-19], and thiazoles [20, 21], are often used as corrosion inhibitors to protect copper and achieve the desired protective effect.

1-Ethyl-5-Mercapto Tetrazole (EMTT) is often used in the pharmaceutical industry as a simple, non-toxic organic molecule. The EMTT molecule contains multiple N and S atoms and has great potential to be an effective corrosion inhibitor for copper. Therefore, in this work, the protective effect of EMTT molecule on copper surface in sulfuric acid solution was investigated. The inhibition performance of EMTT molecule on copper corrosion was evaluated by electrochemical means and observation of surface morphology. The adsorption mode of EMTT molecule on copper surface was investigated, and the relationship between molecular structure and adsorption mechanism was theoretically studied by quantum chemical calculations.

2. EXPERIMENTAL

2.1 Chemicals

The chemical reagents used in the experiment are all analytical grade. Chemical structure of 1-Ethyl-5-Mercapto Tetrazole (EMTT, purity $\geq 99\%$, Adamas-beta, China), Sodium chloride (99.5wt%, Aladdin Chemical Co., Shanghai, China), was used with no further purification. 0.5M dilute sulfuric acid solution is used as corrosive medium. Dissolve sodium chloride. Fig. 1 shows the molecular structure of EMTT. Q235 steel with 99.9 iron content was used as the working electrode with a working area of 1 cm^2 . Before the experiment, they were treated with 400, 800, 1200, 1500, and 2000 sandpaper in sequence.

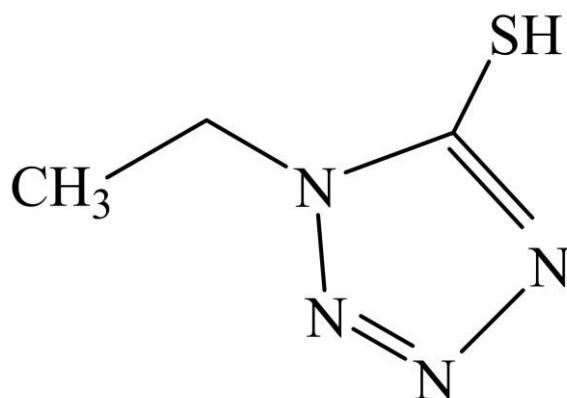


Figure 1. Chemical structure of 1-Ethyl-5-Mercapto Tetrazole

2.2 Electrochemical experiment

Electrochemical experimental tests were carried out using a three-electrode system with a copper specimen as the working electrode, a platinum sheet as the counter electrode and a saturated calomel electrode as the reference electrode. For the electrochemical experiments, the open circuit potential was tested for 1800 s. After it was stabilized, the electrochemical impedance spectrum was tested in the range of 100000 to 0.01 Hz. The impedance parameters were analyzed by fitting curves with Zsimpwin

software. The polarization curve was tested from -0.25V to 0.25V (Vs OCP), with a scan rate of 1 mV/s . All electrochemical experiments were repeated three times to ensure that the results were reliable.

2.3 Surface Analysis

The surface morphology of copper specimens immersed in solutions without and with EMTT corrosion inhibitors for ten hours was examined by SEM (ZEISS MERLIN, 15 kV).

2.4 Density function theory calculation

Dmol3 software was used to investigate quantum chemical calculations. The optimized molecular structure of neutral and protonated EMTT was obtained by density function theory (DFT) using the GGA-BLYP level for the DNP basis set. Associated quantum chemical parameters are also considered: the energy of the frontier molecular orbitals (E_{HOMO} , E_{LUMO}), the energy gap ΔE , and the dipole moment (μ).

3. RESULTS AND DISCUSSION

3.1 Electrochemical testing

Fig. 2 shows the OCP curves for copper in $0.5\text{ M H}_2\text{SO}_4$ without and with EMTT at 298K .

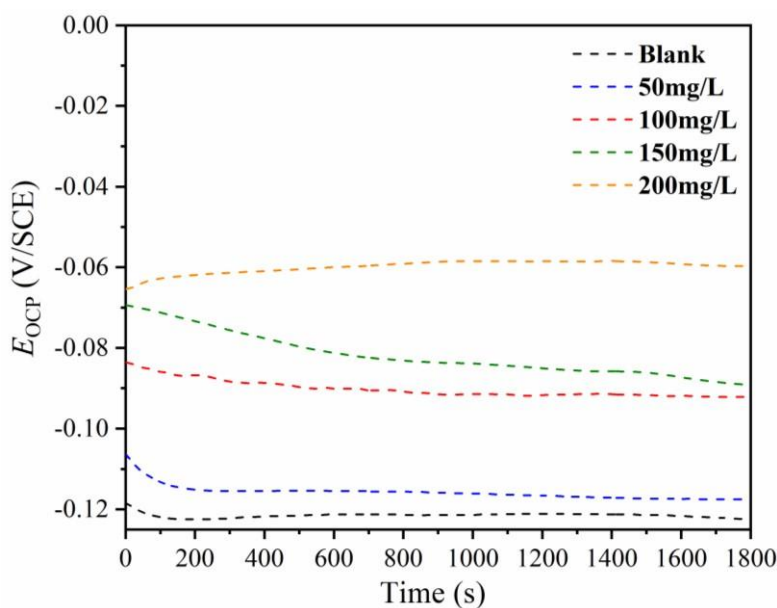


Figure 2. OCP curves for copper in $0.5\text{ M H}_2\text{SO}_4$ without and with EMTT at 298K

According to the curves in the Fig. 2, the OCP value of copper is relatively stable in sulfuric acid solutions. As the EMTT corrosion inhibitor was added to the sulfuric acid solution, the OCP values moved in a positive direction, where the OCP value changed the most after the addition of 200 mg/L, with a difference of 60 mV. This change in behavior might be due to the EMTT molecules adsorbing on the surface of the copper specimen, hindering the attack of aggressive ions [22, 23].

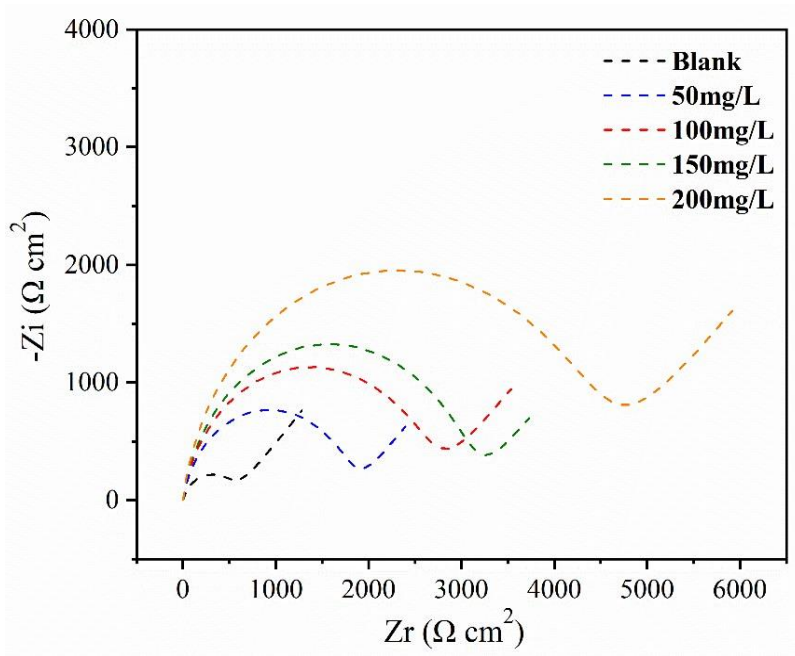


Figure 3. Nyquist plots for copper in 0.5 M H₂SO₄ without and with EMTT at 298K

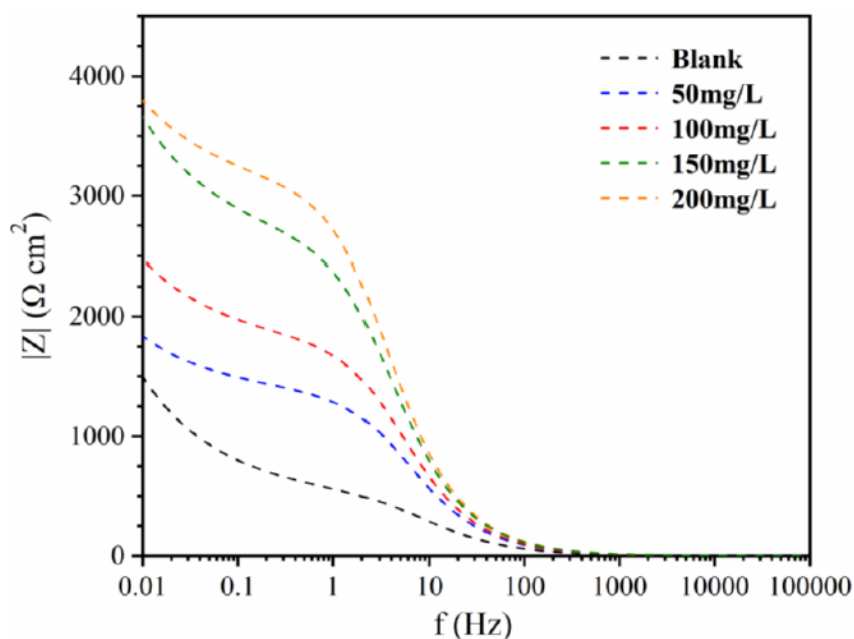


Figure 4. Bode plots for copper in 0.5 M H₂SO₄ without and with EMTT at 298K

Following the OCP tests, the electrochemical impedance spectroscopy (EIS) tests were performed to evaluate the protection of copper by the addition of EMTT corrosion inhibitor in sulfuric acid solutions. Fig. 3 shows Nyquist plots for copper measured in the absence and presence of EMTT molecules in 0.5 M H₂SO₄ solution. As can be seen from the graph, the shape of the Nyquist plot does not change regardless of the presence or absence of inhibitor in the solution, showing two distinct relaxation processes. The semicircle in the high frequency range is attributed to interfacial charge transfer reactions, while the Warburg impedance observed in the low frequency range is related to the diffusion of corrosive species towards or away from the copper electrode [24, 25]. In addition, as the concentration of EMTT added increases, the semicircle diameter increases, indicating a more pronounced protective effect on the copper electrode [26].

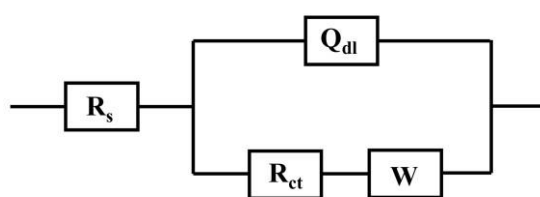


Figure 5. Equivalent circuit model of the copper electrodes in 0.5 M H₂SO₄ solution

The equivalent circuit in Fig. 5 was used to fit the impedance data of the copper specimen. In the circuit, R_s presents the solution resistance, R_{ct} is the charge transfer resistance, and W stands for Warburg impedance. Constant phase element (CPE) is used instead of capacitive components. The impedance of CPE is described as follows:

$$Z_{cpe} = 1 / (Y_0(j\omega)^n) \tag{1}$$

where j : the imaginary root, ω : the angular frequency, Y_0 : proportional factor, and n : the CPE index associated with the inherent chemical and physical heterogeneous characters of the solid surfaces [27-29]. The CPE can show a resistor ($n = 0$), a Warburg impedance ($n = 0.5$), or a capacitor ($n = 1$).

Table 1. Electrochemical impedance parameters obtained for copper in 0.5 M H₂SO₄ without and with EMTT at 298K

C (mg/L)	R_s ($\Omega \text{ cm}^2$)	R_{ct} ($\Omega \text{ cm}^2$)	CPE ($10^{-5} \Omega^{-1} \text{ s}^n \text{ cm}^{-2}$)	W^{-3}	n	η (%)
	1.4	542	8.46	3.7	0.82	
50	1.5	1928	3.33	4.6	0.89	71.90
100	1.3	2634	2.87	3.1	0.89	79.43
150	1.5	3073	2.62	4.2	0.90	82.37
200	1.3	4401	2.20	1.8	0.91	87.69

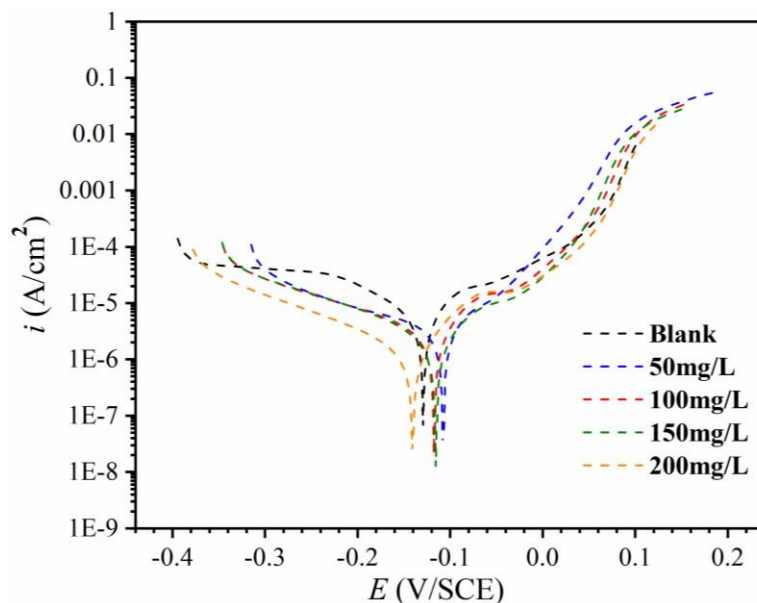


Figure 6. Potentiodynamic polarization curves for copper in 0.5 M H₂SO₄ solution without and with EMTT at 298K

The relevant parameters for impedance are listed in Table 1. The inhibition efficiency can be calculated by the following equation:

$$\eta (\%) = (R_{ct} - R_{ct}^0) / R_{ct} \times 100\% \quad (2)$$

where R_{ct} and R_{ct}^0 are the transfer resistances in the presence and absence of EMTT, respectively. It is clear that copper corrosion was inhibited by the presence of EMTT in the sulfuric acid solution. As the concentration of EMTT in the sulfuric solution increases, the values of CPE are gradually decreasing and the values of R_{ct} is gradually increasing. The optimum inhibition efficiency was achieved with the addition of 200 mg/L EMTT at 87.69%. The results indicate that the EMTT molecules adsorbed on the surface of the copper electrodes and protected them from corrosion.

Fig. 6 shows the potentiodynamic polarization curves for copper in the absence and presence of various concentrations of EMTT corrosion inhibitor in 0.5 M H₂SO₄ solution. As can be seen from the polarization curves, the addition of corrosion inhibitor had a lesser effect on the cathode and a more significant effect on the dissolution of copper in the anode. This is consistent with the smaller change in cathode slope and the larger change in the slope of the anode in Table 2.

The electrochemical parameters such as corrosion potential (E_{corr}), corrosion current density (i_{corr}), anodic (β_a), cathodic (β_c) Tafel slopes were shown in Table 2. The percentage inhibition efficiency η % is given by the following equation (3):

$$\eta (\%) = (i_{corr,0} - i_{corr}) / (i_{corr,0}) \times 100\% \quad (3)$$

It is also known from Table 2 that as the EMTT concentration increases, the corrosion current density gradually decreases and the corrosion inhibition efficiency gradually increases, with the optimum efficiency reaching 88.30% at a concentration of 200 mg/L. The value of E_{corr} was less than 85 mV in all added concentration ranges, so EMTT was considered as a mixed type corrosion inhibitor.

Table 2. The polarization parameters obtained for copper in 0.5 M H₂SO₄ without and with EMTT at 298K

C (mg/L)	E_{corr} (mV/SCE)	i_{corr} ($\mu\text{A cm}^{-2}$)	β_a (mV dec ⁻¹)	β_c (mV dec ⁻¹)	η (%)
	-113	8.36	11	-104	
50	-108	2.09	59	-87	75.00
100	-118	1.66	49	-82	80.12
150	-130	1.37	55	-101	83.60
200	-141	0.98	54	-91	88.30

3.2 SEM analysis

To verify the durability of the corrosion inhibitor, copper specimens were immersed in sulfuric acid solution without and with EMTT corrosion inhibitor for ten hours and the surface morphology was observed. As can be seen in Fig. 7a, the bare copper surface was severely corroded and showed a large number of etched pits. Compared to the bare copper surface, the surface of copper specimen was smoother and flatter with the addition of EMTT to the sulfuric acid solution, and the scratches were still clearly visible. The surface morphology results indicated that EMTT has a good inhibition effect, which is consistent with the electrochemical results.

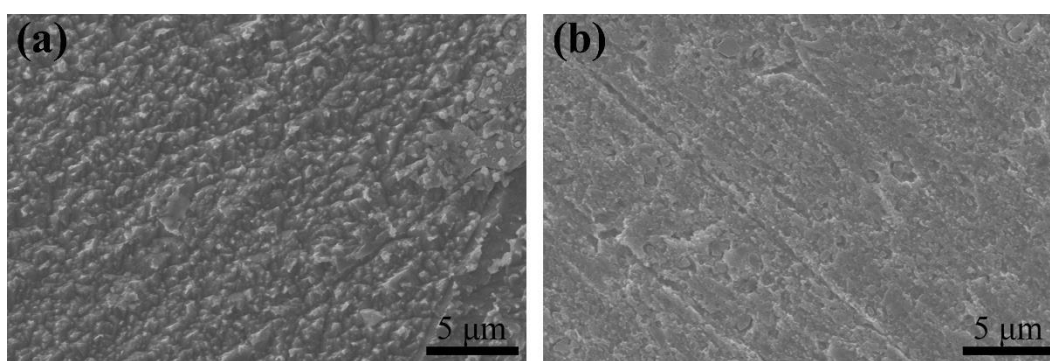


Figure 7. SEM images of bare copper (a) and with 200 mg/L EMTT (b) after being immersed in 0.5 M H₂SO₄ solution for 10h

3.3 Adsorption isotherm

The adsorption behavior of EMTT molecules on copper surfaces was evaluated using the

Langmuir isothermal adsorption model. The Langmuir adsorption isotherm equation is as follows [30]:

$$C/\theta = 1/K_{ads} + C \quad (4)$$

where C is the concentration of the inhibitor, K_{ads} represents the adsorption equilibrium constant, and θ (surface coverage) is defined as the corrosion inhibition efficiency obtained from the polarization curve measurements.

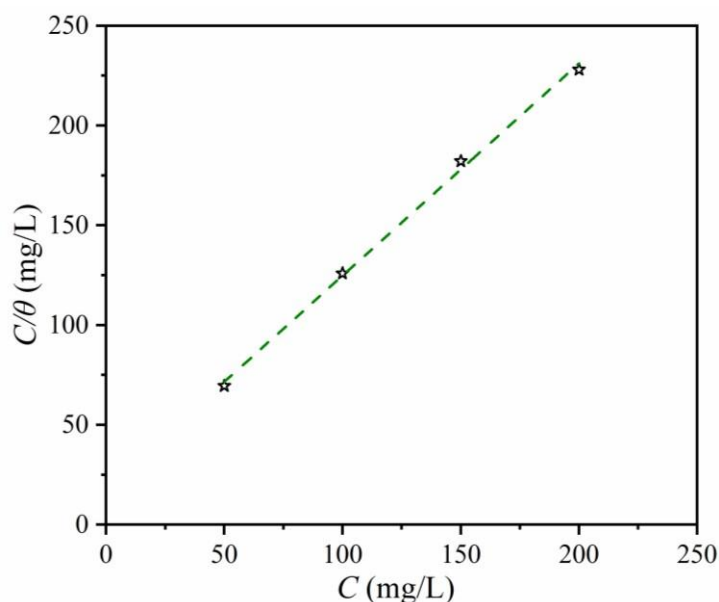


Figure 8. Langmuir adsorption plots of EMTT on the copper electrodes in 0.5 M H₂SO₄ solution

The fitted Langmuir adsorption isotherm plot is shown in Fig. 8, where the slope is 1.06 and the regression coefficient (R^2) is close to 1, which indicates that the adsorption of EMTT on the copper surface follows the Langmuir adsorption isotherm. The free energy of adsorption ΔG^0_{ads} was calculated as follows:

$$K_{ads} = 1/C_s \exp\left(\frac{-\Delta G^0_{ads}}{RT}\right) \quad (5)$$

Herein, R is the molar gas constant ($8.314 \text{ J mol}^{-1} \text{ K}^{-1}$) and T is the absolute temperature (K), C_s corresponds to the concentration of water in solution ($1 \times 10^3 \text{ g/L}$). The calculated Gibbs free energy is about $-27.01 \text{ kJ mol}^{-1}$. According to the literature, it is known that ΔG^0_{ads} is both physical and chemical adsorption in the range of -40 kJ mol^{-1} to -20 kJ mol^{-1} . Based on the above results, it is clear that EMTT adsorption on copper surfaces in sulfuric solution is both physical and chemical [31, 32].

3.4 Quantum chemical study

To investigate the mechanism of adsorption of EMTT molecule on copper, quantum chemical calculations were carried out on the neutral and protonated molecule. Fig. 9 shows the optimal structures of EMTT neutral and protonated molecule, ESP, HOMO and LUMO. As can be seen from the figure, the HOMO distribution positions of the neutral and protonated EMTT molecule are almost identical, located at the tetrazole and its sulfhydryl group. The LUMO distribution is basically similar to HOMO, also concentrated at the tetrazole and sulfhydryl positions. In addition, it can be seen from the ESP diagram that the yellow (negative) regions associated with nucleophilic reactions in the EMTT neutral molecule are mainly located on the tetrazolium N atoms, which readily interact with the Cu surface [22, 33, 34]. The blue regions of the EMTT protonated molecule with electrophilic reactivity are distributed over the entire protonated molecule.

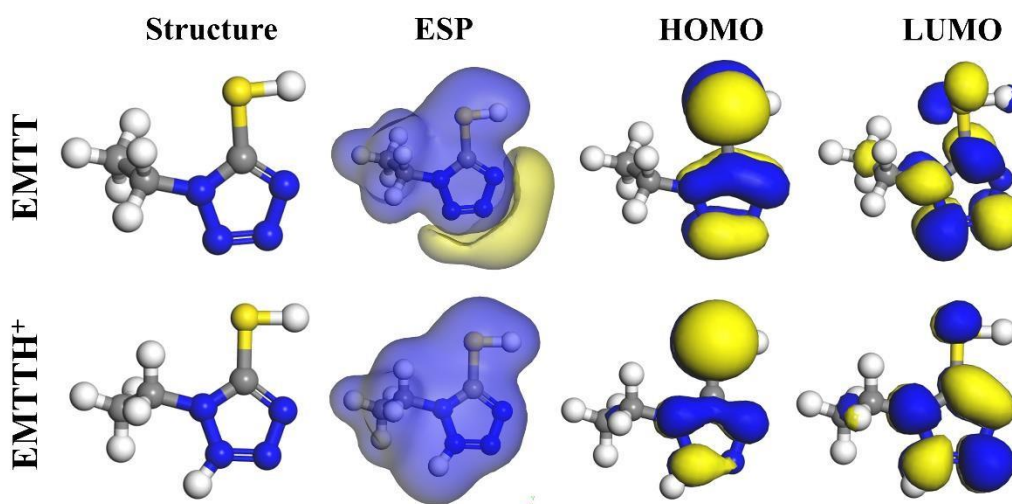


Figure 9. The structure, ESP, HOMO and LUMO neutral and protonated EMTT molecule

It is known that HOMO contributes to the electron-donating ability of molecules, while LUMO contributes to the electron-receiving ability of molecules [35]. The larger the HOMO value, the greater the electron donating ability of the molecule; conversely, the LUMO value is small, the electron reception ability is stronger [36]. Therefore, the energy gap value ($\Delta E = E_{LUMO} - E_{HOMO}$) and the dipole moment value, another important quantum chemical parameter, are usually used to determine the inhibitory ability of corrosion inhibitors [37, 38]. It is generally accepted that a smaller dipole moment facilitates better corrosion inhibition by the molecule. As shown in Table 3, EMTT neutral and protonated molecules have large energy gap values and small dipole moment values, indicating a stronger inhibitory effect.

Table 3. The HOMO and LUMO energy, energy gap, and μ for neutral and protonated molecule

Molecule	E_{HOMO} (eV)	E_{LUMO} (eV)	ΔE (eV)	μ (D)
EMTT	-6.07	-1.42	4.65	5.48
EMTTH+	-11.20	-7.78	3.42	14.52

4. CONCLUSION

In summary, the protective properties of a commonly used drug molecule against copper in sulfuric acid media were evaluated. The electrochemical results clearly showed that the protection of the copper surface is significantly enhanced when EMTT molecule is added to the sulfuric acid solution. There was a positive correlation between the inhibition efficiency and the concentration of EMTT added, and the best inhibition efficiency 88.30% was achieved at the content of 200 mg/L. The surface morphology observed by SEM supported the conclusions drawn from the electrochemical experiments.

By fitting the adsorption model, it was shown that the adsorption model of EMTT molecule on copper is consistent with the Langmuir model and is a combination of physical and chemical adsorption. Eventually, quantum chemical calculations on the EMTT neutral and protonated molecules have been carried out to explain theoretically why they can be used as corrosion inhibitors for copper.

References

1. H. Hammache, L. Makhloufi, B. Saidani, *Corros. Sci.*, 45 (2003) 2031-2042.
2. K.F. Khaled, N. Hackerman, *Electrochim. Acta.*, 49 (2004) 485-495.
3. H. Li, S. Zhang, Y. Qiang, *J. Mol. Liq.*, 321 (2021) 114450.
4. Y. Qiang, L. Guo, H. Li, X. Lan, *Chem. Eng. J.*, 406 (2021) 126863.
5. Marija B. Petrović Mihajlović, Milan M. Antonijević, *Int. J. Electrochem. Sci.*, 10 (2015) 1027-1053.
6. Marija B. Petrović, Ana T. Simonović, Snežana M. Milić, Milan M. Antonijević, *Int. J. Electrochem. Sci.*, 7 (2012) 9043-9057.
7. Y. Qiang, S. Zhang, S. Xu, L. Yin, *Rsc Adv.*, 5 (2015) 63866-63873.
8. G. Bahlakeh, A. Dehghani, B. Ramezanzadeh, M. Ramezanzadeh, *J. Mol. Liq.*, 293 (2019) 111559.
9. A. Dehghani, G. Bahlakeh, B. Ramezanzadeh, *Bioelectrochemistry.*, 130 (2019) 107339.
10. S.A.A. El-Maksoud, *Electrochim. Acta.*, 49 (2004) 4205-4212.
11. L. Larabi, O. Benali, S.M. Mekelleche, Y. Harek, *Appl. Surf. Sci.*, 253 (2006) 13711378.
12. H. Otmacic Curkovic, E. Stupnisek-Lisac, H. Takenouti, *Corros. Sci.*, 52 (2010) 398405.
13. K.F. Khaled, *Electrochim. Acta.*, 54 (2009) 4345-4352.
14. Sudheer, M.A. Quraishi, *Corros. Sci.*, 70 (2013) 161-169.
15. E.-S.M. Sherif, R.M. Erasmus, J.D. Comins, *Corros. Sci.*, 50 (2008) 3439-3445.
16. Y. Qiang, H. Li, X. Lan, *J. Mater. Sci. Technol.*, 52 (2020) 63-71.
17. Y. Qiang, S. Zhang, S. Xu, W. Li, *J. Colloid. Interf. Sci.*, 472 (2016) 52-59.
18. Y. Qiang, S. Zhang, L. Guo, X. Zheng, B. Xiang, S. Chen, *Corros. Sci.*, 119 (2017) 68-78.
19. Y. Qiang, S. Zhang, S. Yan, X. Zou, S. Chen, *Corros. Sci.*, 126 (2017) 295-304.
20. E.M. Sherif, S.-M. Park, *Electrochim. Acta.*, 51 (2006) 6556-6562.
21. Y. Qiang, S. Xu, L. Guo, N. Chen, Ime B. Obot, *Int. J. Electrochem. Sci.*, 11 (2016) 3147-3163.
22. Z. Chen, Z. Liu, K. He, G. Han, Y. Lv, J. Han, X. Wei, *Int. J. Electrochem. Sci.*, 16 (2021) 210559.

23. H. Li, Y. Qiang, W. Zhao, S. Zhang, *Corros. Sci.*, 191 (2021) 109715.
24. Y. Qiang, S. Zhang, L. Guo, S. Xu, L. Feng, I.B. Obot, S. Chen, *J. Clean. Prod.*, 152 (2017) 17-25.
25. Y. Qiang, S. Fu, S. Zhang, S. Chen, X. Zou, *Corros. Sci.*, 140 (2018) 111-121.
26. M. Prabakaran, S.-H. Kim, N. Mugila, V. Hemapriya, K. Parameswari, S. Chitra, I.-M. Chung, *J. Ind. Eng. Chem.*, 52 (2017) 235-242.
27. Y. Qiang, S. Zhang, Q. Xiang, B. Tan, W. Li, S. Chen, L. Guo, *Rsc Adv.*, 8 (2018) 38860-38871.
28. M. Tabatabaei majd, G. Bahlakeh, A. Dehghani, B. Ramezanzadeh, M. Ramezanzadeh, *J. Mol. Liq.*, 291 (2019) 111281.
29. M.T. Majd, M. Ramezanzadeh, B. Ramezanzadeh, G. Bahlakeh, *J. Hazard. Mater.*, 382 (2020) 121029.
30. S. Pareek, D. Jain, S. Hussain, A. Biswas, R. Shrivastava, S.K. Parida, H.K. Kisan, H. Lgaz, I.-M. Chung, D. Behera, *Chem. Eng. J.*, 358 (2019) 725-742.
31. Y. Qiang, S. Zhang, L. Wang, *Appl. Surf. Sci.*, 492 (2019) 228-238.
32. Y. Qiang, S. Zhang, H. Zhao, B. Tan, L. Wang, *Corros. Sci.*, 161 (2019) 108193.
33. P. Dohare, K.R. Ansari, M.A. Quraishi, I.B. Obot, *J. Ind. Eng. Chem.*, 52 (2017) 197210.
34. Y. Qiang, S. Zhang, B. Tan, S. Chen, *Corros. Sci.*, 133 (2018) 6-16.
35. M. Ramezanzadeh, G. Bahlakeh, B. Ramezanzadeh, *J. Mol. Liq.*, 292 (2019).
36. S. Issaadi, T. Douadi, S. Chafaa, *Appl. Surf. Sci.*, 316 (2014) 582-589.
37. L. Guo, S. Kaya, I.B. Obot, X. Zheng, Y. Qiang, *J. Colloid. Interf. Sci.*, 506 (2017) 478485.
38. L. Guo, I.B. Obot, X. Zheng, X. Shen, Y. Qiang, S. Kaya, C. Kaya, *Appl. Surf. Sci.*, 406 (2017) 301-306.

© 2022 The Authors. Published by ESG (www.electrochemsci.org). This article is an open access article distributed under the terms and conditions of the Creative Commons Attribution license (<http://creativecommons.org/licenses/by/4.0/>).